International Journal of Modern Physics C

LATTICE BOLTZMANN SIMULATION ON FLOW WITH SOOT ACCUMULATION IN DIESEL PARTICULATE FILTER

KAZUHIRO YAMAMOTO, SHINGO SATAKE and HIROSHI YAMASHITA

Department of Mechanical Engineering, Nagoya University
Furo-cho, Chikusa-ku, Nagoya, Aichi 464-8603, Japan
kazuhiro@mech.nagoya-u.ac.jp

NAOKI TAKADA and MASAKI MISAWA

National Institute of Advanced Industrial Science and Technology (AIST)
1-2-1 Namiki, Tsukuba, Ibaraki 305-8564, Japan

Received 1 November 2006
Revised 15 January 2007

Since diesel exhaust gas has more ambient air pollutants such as NOx and particulate matters (PM) including soot, the special treatment for exhaust emission standards is needed. Recently, a diesel particulate filter (DPF) has been developed to reduce PM in the after-treatment of exhaust gas. However, since the structure of the filter is small and complex, it is impossible to examine the phenomena inside the filter experimentally. In this study, we conduct fluid simulation in the diesel filter. We use the lattice Boltzmann method. The soot accumulation is considered to simulate the PM trap in the filter. For the wall-boundary in the simulation, the inner structure of the filter is obtained by a 3D-CT technique. Results show complex flow pattern in the diesel filter. Due to the soot accumulation, the velocity is changed and the pressure is increased. The pressure drop becomes larger as soot concentration at the inlet is higher.

Keywords: Lattice Boltzmann method; Soot; Porous media; Diesel particulate filter

PACS Nos.: 47.11.-j, 47.55.Kf, 47.56.+r, 47.61.-k, 47.70.Fw

1. Introduction

Currently, most commercial vehicles such as cargo trucks, trailers, or buses are powered by a diesel engine. The reason for the wide use of diesel is its high fuel efficiency and durability, and the share of diesel cars including passenger cars in the world is gradually increased. However, diesel exhaust gas has more ambient air pollutants such as oxides of nitrogen (NOx) and particulate matters (PM) including soot, and a significant impact on our environment arises. For this reason, more strict exhaust emission standards such as Euro V in 2008 are setting in many countries. As for the PM emissions, a diesel particulate filter (DPF) has been recently developed. In simple explanation of DPF, it traps the particles when exhaust gas passes its porous

wall. It is the most efficient after-treatment device, attaining filtration efficiencies over 90% under normal operating conditions.[1]

However, the filter would be plugged with particles to cause the increase of fiter back pressure, especially in the case of heavy-duty vehicles. Fitler back pressure must be kept at the lower levels, because it increases fuel consumption and reduces available torque.[2] Then, the accumulated particles must be removed, which are chemically treated, and usually burned in combustion. This is called filter regeneration process. The more advanced system is proposing with catalytic converter for oxidation of deposited particules,[3] which is the passive regeneration process. However, this process only takes place in some temperature range, and it is still in the phase of research and development. So far, it is difficult to observe the phenomena inside the filter experimentally. There are not enough information on the particle accumulation in the filter. To develop DPF effectively, we need to understand the phenomena especially during the process of removing diesel particulates in exhaust gas. Then, it is helpful to simulate the flow in the diesel filter to understand the particle deposition phenomena and predict characteristics of DPF in advance. Recently, by using the lattice Boltzmann method (LBM), we have simulated the flow with particles in porous media.[4,5] In LBM, the treatment of boundary conditions is simple and easy, and it is appropriate to calculate porous media flow.[6−13]

In this study, we conduct lattice Boltzmann simulation for the flow in a real diesel filter. For this purpose, we use a micro-Focus X-ray CT technique. One of the advantages of tomography-assisted simulation is to be able to estimate local velocity and pressure distributions in micro structure inside the real sample, where hardly any measurement techniques are available. Non-destructive nature of the CT technique allows visualization of the solid structure of a diesel filter actually used. The filter used is shown in Fig.1, which is produced by COTEC Limited, Japanese company in Nagoya city. We discuss the flow pattern and pressure change caused by soot accumulation.

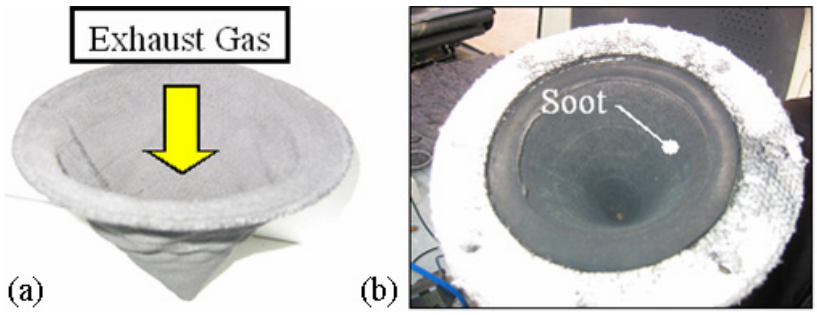

Fig. 1. (a) Diesel filter produced by COTEC Ltd, (b) soot removed by the diesel filter.

2. Numerical Method

We have developed numerical scheme for simulating fluid with soot accumulation in porous media.[4,5]. For flow field, the incompressible lattice BGK model of D3Q15 [10] is used. The evolution equation using the pressure distribution function, F_P, is,

$$F_{P,\alpha}(\mathbf{x}+\mathbf{e}_\alpha\delta_t, t+\delta_t) - F_{P,\alpha}(\mathbf{x},t) = -\frac{1}{\tau_P}[F_{P,\alpha}(\mathbf{x},t) - F^{eq}_{P,\alpha}(\mathbf{x},t)], \quad (1)$$

where δ_t is the time step, and τ_P is the relaxation time that controls the rate of approach to equilibrium. The equilibrium distribution function, $F^{eq}_{P,\alpha}$, is given by

$$F^{eq}_{P,\alpha} = w_\alpha \left\{ p + p_0 \left[3\frac{\mathbf{e}_\alpha\cdot\mathbf{u}}{c^2} + \frac{9}{2}\frac{(\mathbf{e}_\alpha\cdot\mathbf{u})^2}{c^4} - \frac{3}{2}\frac{\mathbf{u}\cdot\mathbf{u}}{c^2} \right] \right\}, \quad (2)$$

where w_α=1/9 (α=1:6), w_α=1/72 (α=7:14), and w_{15}=2/9. The sound speed, c_s, is $c/\sqrt{3}$ with p_0=$\rho_0 RT$=$\rho_0 {c_s}^2$. Here, p_0 and ρ_0 are the pressure and density at the standard ambient temperature and pressure. The pressure and local velocity of $\mathbf{u}$=(u_x, u_y, u_z) are obtained by the following equations.

$$p = \sum_\alpha F_{P,\alpha} \quad (3)$$

$$\mathbf{u} = \frac{1}{p_0}\sum_\alpha \mathbf{e}_\alpha F_{P,\alpha} \quad (4)$$

The relaxation time is related with the kinetic viscosity using ν=$(2\tau-1)/6c^2\delta_t$.

The soot accumulation is described by the modified particle deposition model.[14] Different from Lagrangian approach through the equation of motion,[15] individual particles are not considered. Instead, the soot concentration is monitored at the surface of filter wall. As the soot accumulation is continued, the soot concentration sometime becomes unity. When this limit is reached, the solid site is piled up. The accumulated soot region is treated as non-slip wall, which implies a dynamically change of boundary condition for fluid. The LB equation for soot mass fraction is,

$$F_{C,\alpha}(\mathbf{x}+\mathbf{e}_\alpha\delta_t, t+\delta_t) - F_{C,\alpha}(\mathbf{x},t) = -\frac{1}{\tau_C}[F_{C,\alpha}(\mathbf{x},t) - F^{eq}_{C,\alpha}(\mathbf{x},t)] + w_\alpha Q_C, \quad (5)$$

where F_C is the distribution function for soot mass fraction and τ_C is the relaxation time determined by diffusion coefficient. The source term, Q_C, is the treatment of soot accumulation around the porous wall surface. For simplicity, soot is thoroughly attached to the porous wall without desorption. The equilibrium distribution function, $F^{eq}_{C,\alpha}$, is given by

$$F^{eq}_{C,\alpha} = w_\alpha Y_C \left\{ 1 + 3\frac{\mathbf{e}_\alpha\cdot\mathbf{u}}{c^2} + \frac{9}{2}\frac{(\mathbf{e}_\alpha\cdot\mathbf{u})^2}{c^4} - \frac{3}{2}\frac{\mathbf{u}\cdot\mathbf{u}}{c^2} \right\}. \quad (6)$$

The mass fraction of soot is obtained by the sum of the distribution function as Y_C=$\Sigma F_{C,\alpha}$. In our previous study,[4] soot accumulation has been well described to observe effect of soot accumulation on flow field, with smaller porosity and larger wetted surface. It has been found that the friction factor with soot accumulation is smaller than the predicted value by the Ergun equation.

3. Results and Discussion

3.1. *Inner structure of diesel filter by 3D X-ray tomography*

For simulating the flow in the real diesel filter, we obtain the inner structure by an X-ray CT technique. A micro-focus X-ray tomography system was developed by Uni-Hite System Corporation, Japan.[16] A piece of diesel filter was scanned by XVA-160, equipped with a 160kVp transmission X-ray source with a focus spot of 1mm and a 4-inch Image Intensifier to capture images by an 8-bit, 640×480 CCD camera.

The imaging conditions were searched to provide optimum contrast in image. Resulting tube voltage and current were 50kV and 900mA, respectively. Magnification factor was set at 7.5, leading to spatial resolution of 11μm/pixel in reconstruction domain. A set of 360 projection images was taken at 1 degree interval during a single rotation. Conventional Feldkamp algorithm with filtered back-projection was used to reconstruct a 512×512×280 3D image. In our previous study,[4] we have tested Ni-Cr porous metal to confirm the applicability of the tomography-assisted simulation.

In the present simulation in real diesel filter, we employed a similar data processing technique. First, we scanned a piece of diesel filter sample and reconstructed 3D binary image. Figure 2(a) shows the cross sectional view in x-y plane. Stack of the cross section images yields the whole shape of the filter piece as shown in Fig.2(b), which resolves the individual fibers in bundles that are woven into a cloth. The actual size of the filter piece is 5.8mm(Length)×3.2mm(Width)×0.73mm(Thickness). The 3D inner structure serves as a boundary condition in the simulation.

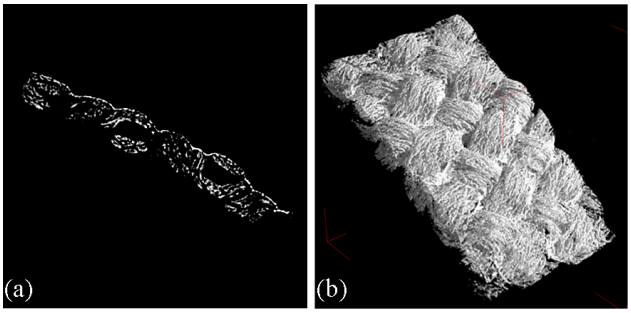

Fig. 2. (a) CT image in x-y plane, and (b) 3D reconstructed computerized image.

3.2. *Fluid simulation*

Figure 3 shows the coordinate and boundary conditions. The calculation domain is 2.25mm×1.35mm×1.35mm, and the inflow velocity, U_{in}, is 10cm/s. The total number of grids is 201×121×121, with grid size of 11μm, which is the same value of

the X-ray CT measurement. The diesel filter of L=0.73mm is placed in the center part in this calculation domain. The number of grid for the filter thickness is 65. In the calculation, all equations are non-dimensionalized based on similarity to obtain the flow and concentration fields. As for the boundary condition, the inflow boundary is adopted at the inlet.[17] At the sidewall, the slip boundary condition is adopted, considering the symmetry.[11] At the outlet, the pressure is constant, and the gradient of soot concentration is zero. On the surface of the porous wall, bounce-back rule for non-slip boundary condition is adopted.

Figure 4 shows non-dimensional velocity in flow direction, u_x/U_{in}. Only x-y plane at the center is shown, with the slice image of the filter in Fig.4(a). The large pore exists inside the filter, and the complex fiber structure is observed. Although the flow at the inlet is uniform, the flow direction is largely changed inside the filter. The velocity is locally different, and the flow is accelerated in the filtration route.

Next, we examine the pressure field, which is shown in Fig.5. This pressure is

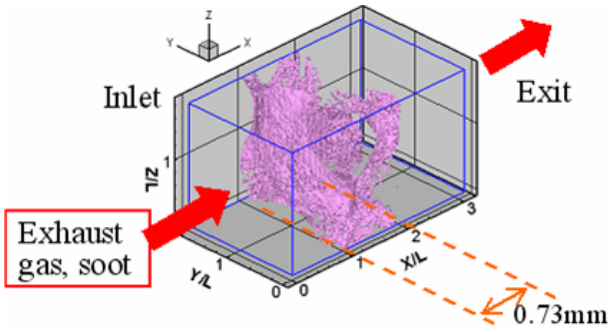

Fig. 3. Coordinate and diesel filter used in the simulation.

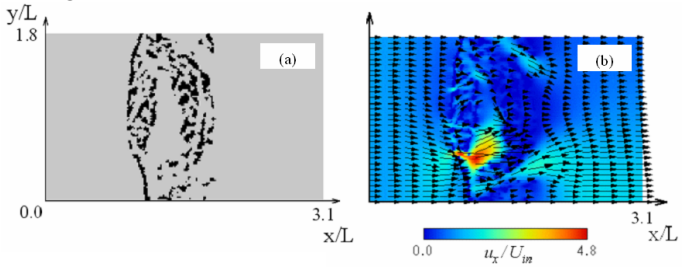

Fig. 4. (a) Slice image of the filter, (b) simulated flow field in x-y plane.

averaged value in the y-z plane. Usually, in homogenous porous media, the pressure gradually decreases in the flow direction, and the constant pressure gradient is observed. However, the pressure gradient in this figure is changed. Here, we check the porosity in x-axis (flow direction) in the calculation domain. The mean porosity in the y-z plane is also shown in Fig.5. The filter is placed in the range of x/L=0.9

to 1.9 in this figure, and the porosity is unity outside this region. The estimated porosity of the filter is roughly from 0.7 to 0.9. It is found that the porosity is largely changed due to non-uniformity of the filter structure. Mainly, there are two regions of low porosity at x/L=1.0 to 1.2 and relatively higher porosity at x/L=1.2 to 1.8 due to the fiber structure of the filter. Then, it is considered that because of the non-uniformity of the porosity, the pressure gradient is changed in these two regions.

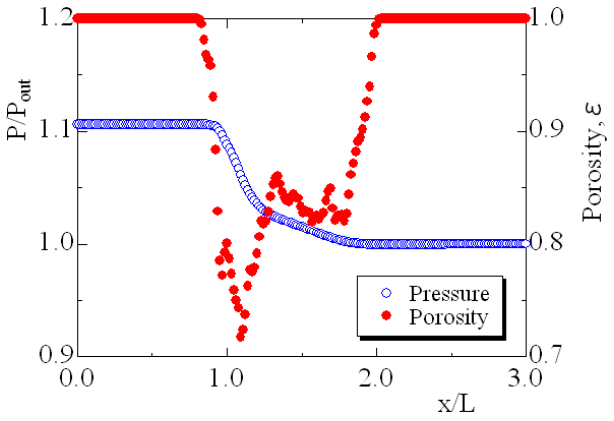

Fig. 5. Pressure and porosity distributions in the diesel filter.

3.3. *Soot accumulation*

Finally, we simulate the flow with soot accumulation. Figure 6 shows accumulated soot in the calculation domain. These profiles are obtained at t=0.225ms and 2.25ms, respectively. The mass fraction of soot at the inlet, $Y_{C,in}$, is 0.1. After the soot is attached to the filter wall surface, the velocity field is changed. That is, the velocity is largely accelerated in the narrow path caused by the soot accumulation. The soot is preferably accumulated upstream.

Figure 7 shows the pressure with soot deposition. The profile is obtained at t=5.0ms. The soot concentration at the inlet is varied. The mass fraction of soot is 0.01, 0.05, 0.075, and 0.1. For comparison, the pressure before soot deposition is also shown. When soot is accumulated, the pressure especially at the inlet is increased. This is because the main region of the soot deposition is around the inlet. The similar pressure change is observed when the deposited layer is developed in the gas-particle flow.[15]

Figure 8 shows the total accumulated soot inside the filter, which is evaluated by the mass of soot per the filter unit volume. The mass fraction of soot at the inlet is 0.01 to 0.1. As the soot concentration is larger, more soot is accumulated inside the filter. Since the porosity inside the filter is largely reduced by the soot

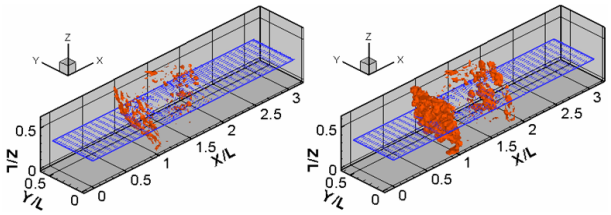

Fig. 6. Soot accumulation with velocity vector: (a) t=0.225ms, (b) t=2.25ms.

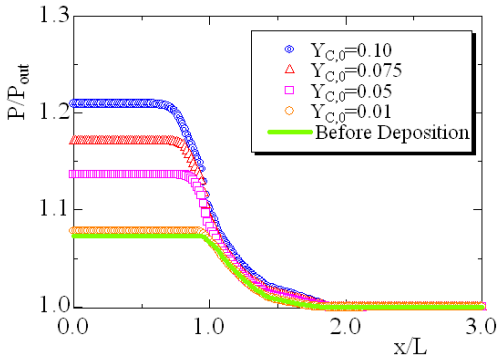

Fig. 7. Pressure change with soot deposition at t=5.0ms.

deposition, the effect of soot deposition appears in the pressure field. That is, more soot is accumulated in the filter, the region available for flow is decreased to cause the higher back pressure across the filter.

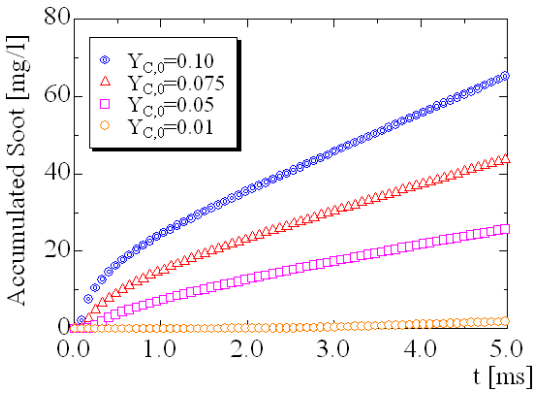

Fig. 8. Accumulated soot inside the filter at different soot concentration at the inlet.

4. Conclusions

We have conducted LB simulation on flow with soot accumulation in real diesel filter (DPF). Inner structure of the filter is analyzed by 3D X-ray CT. Results show that:

(i) The estimated porosity of the filter is approximately from 0.7 to 0.9. Due to the fiber structure of the filter, the porosity varies. Resultantly, the pressure gradient along the flow direction is not constant.
(ii) Soot accumulation mainly occurs at the inlet of the filter. Flow and pressure changes due to smaller porosity.
(iii) As soot concentration at the inlet is higher, accumulated soot is increased, with filter backpressure larger.

This information is useful for understanding the phenomena in the diesel filter to predict the filter characteristics for the better design of DPF.

Acknowledgments

This work was partially supported by New Energy and Industrial Technology Development Organization (Industrial Technology Research Grant, 05A18020d) in Japan. The filter sample was offered by COTEC Ltd. in Japan.

References

1. J. C. Clerc, *Appl. Catal. B-Environ.* **10**, 99 (1996).
2. A. M. Stamatelos, *Energy Conv. Manag.* **38**, 83 (1997).
3. G. A. Stratakis and A. M. Stamatelos, *Combust. Flame* **132**, 157 (2003).
4. K. Yamamoto, S. Satake, H. Yamashita, N. Takada, and M. Misawa, *Math. Comput. Simul.* **72**, 257 (2006).
5. K. Yamamoto and F. Ochi, *J. Energy Inst.* **79**, 195 (2006).
6. G. McNamara and G. Zanetti, *Phys. Rev. Lett.* **61**, 2332 (1988).
7. F. J. Higuera, S. Succi, and R. Benzi, *Europhys. Lett.* **9**, 345 (1989).
8. S. Succi, E. Foti, and F. Higuera, *Europhys. Lett.* **10**, 433 (1989).
9. A. Cancelliere, C. Chang, E. Foti, D. H. Rothman, and S. Succi, *Phys. Fluids A* **2**, 2085 (1990).
10. Y. H. Qian, D. d'Humie'res, and P. Lallemand, *Europhys. Lett.* **17**, 479 (1992).
11. T. Inamuro, M. Yoshino, and F. Ogino, *Int. J. Numer. Meth. Fluids* **29**, 737 (1999).
12. J. Bernsdorf, G. Brenner, and F. Durst, *Comput. Phys. Commun.* **129**, 247 (2000).
13. M. Yoshino and T. Inamuro, *Int. J. Numer. Meth. Fluids* **43**, 183 (2003).
14. B. Chopard, A. Masselot, and A. Dupuis, *Comput. Phys. Commun.* **129**, 167 (2000).
15. O. Filippova and D. Hänel, *Comput. Fluids* **26**, 697 (1997).
16. M. Misawa, I. Tiseanu, R. Hirashima, K. Koizumi, and Y. Ikeda, *Key Eng. Mater.* **270**, 1135 (2004).
17. Q. Zou and X. He, *Phys. Fluids* **9**, 1591 (1997).